Development and Characterization of Novel Freeze-thawed Polyvinyl Alcohol/ Halloysite Hydrogels

An approach for drug delivery application

ADI GHEBAUR[1]*, SORINA ALEXANDRA GAREA[1], SERGIU CECOLTAN[1], HORIA IOVU[1,2]

[1] University Polytehnica of Bucharest, Advanced Polymer Materials Group, 1-7 Gheorghe Polizu Str., 011061, Bucharest, Romania

[2]Academy of Romanian Scientists

The influence of aluminosilicates on the structure and drug release profiles of polyvinyl alcohol (PVA) – halloysite (HNT) hydrogels containing acetylsalicylic acid (ASA) as a model drug was monitored. The hydrogels were synthesized using a three cycle freeze – thawing procedure and were characterized by FTIR, XRD and SEM. The swelling degree and cytotoxicity were also determined. All hydrogels properties were influenced by HNT concentration from the polymer matrix. The release of ASA, from PVA – HNT hydrogels was monitored in the gastrointestinal tract conditions.

Keywords: freeze-thawing, halloysite, acetylsalicylic acid, polyvinyl alcohol

Hydrogels are materials, with a three-dimensional structure obtained by polymer crosslinking, able to absorb a high amount of water or aqueous biological fluids [1]. Due to the fact that they are characterized by a high swelling degree, hydrogels have been widely used in biomedical field such as drug delivery [2], tissue engineering [3], biosensors [4] etc. Regarding the drug delivery systems, hydrogels not only reduce the speed release of drugs but also act as a carrier to the site of action, drug molecules being loaded within the gaps formed between the crosslinked polymer networks. Once the system is administered within the body, the drug diffuses through the swelled hydrogel [5].

The curing of hydrogels can be performed by various methods: physical crosslinking using a thermal treatment (heating or freeze-thawing), electrostatic interaction, hydrophobic interactions, hydrogen bonding interactions, stereocomplexation or irradiation (UV, gamma-ray) [6-10] and chemical cross-linking [11, 12]. Among these, freeze-thawing crosslinking process is preferred in biomedical and pharmaceutical field being a biocompatible process. Compared to a hydrogel obtained by chemical cross-linking, the freeze-thawing treatment has the ability to achieve a biomaterial with a rubbery nature and a higher absorption capacity [13]. By controlling some crosslinking parameters like the number of freeze-thawing cycles, the freezing and thawing temperatures and times can be controlled the properties of the hydrogels [14, 15].

However, hydrogels exhibit two major drawbacks that limit their applicability as drug delivery systems: low mechanical properties and a poor adsorption capacity. These may be enhanced by adding different types of aluminosilicates like montmorillonite, layered double hydroxide, smectite, halloysite [16-20] etc. From all aluminosilicates, halloysite exhibits a unique structure characterized by a hallow tubular shape similar with the one of carbon nanotubes. Halloysite exhibits a bivalent morphology where the silanol groups (Si-OH) from the external surface are negatively charged, while the aluminol groups (Al-OH) from the internal surface are positively charged in low pH solutions (pH 2-8) and are negatively charged in high pH solutions (*p*H 9-12) [21]. Thus halloysite can be dispersed in low or high polar polymers [22-24] like polyamide, chitosan, polyacrylamide, polylactide, elastomer [25-33].

In drug delivery field halloysite is intensively used because it presents a lumen where different types of active substances could be loaded and so the clay acts as a carrier [34-37]. The major drawback of this clay is the low loading capacity and a fast drug release, because the active substances interacts through hydrogen bonds with the hydroxyl groups from halloysite [34]. These drawbacks can be cancelled by dispersing the aluminosilicate within the polymer matrix. For instance the interaction between the polyvinyl alcohol (PVA) and the clay surface takes place between the hydroxyl groups from the polymer and the oxygen atoms from clays and forms strong hydrogen bonds.

The aim of this study is to develop halloysite (HNT) based polyvinyl alcohol (PVA) hydrogels used for oral administration. As a model drug acetylsalicylyic acid (ASA) was used. These novel hybrid materials were characterized by different techniques like FTIR, XRD, SEM. Also the influence of clay concentration onto the swelling degree, cytotoxicity, drug release profiles and the drug release mechanism was investigated.

Experimental part

Materials and methods

Acetylsalicylic acid (ASA), polyvinyl alcohol (PVA) with 98–99% hydrolysis degree and a typical molecular weight 31,000–50,000 g/mol, and halloysite nanoclay (HNT) with a diameter between 30 and 70 nm, a length of 1.3μm, a pore size volume of 1.26–1.34 mL/g, a surface area of 64 m^2/g and a cation exchange capacity of 8 mequiv/100 g were purchased from Sigma–Aldrich. All materials were used without further purification. The reagents 3-(4,5-dimethylthiazol- 2-yl)-2,5-diphenyltetrazolium bromide (MTT), Dulbecco's modified eagle medium (DMEM) from Merk Millipore suplimented with 2mM L-glutamine, fetal bovine serum (FBS) from biochrom, 0.05% Trypsin EDTA solution from Merk Millipore, DMSO and phosphate buffer saline (PBS, *p*H = 7.4) from Sigma Aldrich were used for cell viability assays.

* *email: ghebauradi@yahoo.com; Phone: +40214022726*

Hydrogel preparation

PVA aqueous solution (5 wt. %) was prepared by solubilization of PVA powder in distilled water at 90°C. Different amounts of HNT (1, 5 and 10 wt. %) were dispersed into the PVA solution and ultrasonicated for 30 min at room temperature in order to gain a homogenous suspension which was then casted onto Petri dishes and frozen for 24 h at -20 °C. After that they were thawed for 3 h at 30°C in order to achieve the crosslinking process. This cycling process was repeated three times. The samples were dried at room temperature for 48 h. In order to determine the drug delivery potential of PVA/HNT hydrogels, ASA was used as a model drug. For synthesis of this type of hydrogels, that include ASA, 1 wt. % of ASA reported at pure PVA was introduced in the mixture, before sonication. Then the hydrogels were obtained using the same freeze-thawing procedure and further used in release characterization with no adjustments. The samples were dried at room temperature for 48 h.

Characterization

FTIR analysis

FTIR spectra were recorded on a Bruker VERTEX 70 spectrometer using 32 scans with a resolution of 4 cm^{-1} in 4000–600 cm^{-1} region using an ATR modulus.

X-ray diffraction analysis

The XRD curves of the films were registered on a PanalyticalX'Pert Pro MPD instrument with a CuKα radiation (λ=1.5418 Å) over a range of 2θ= 1°– 30° angle.

Swelling measurements

The swelling degree of the hydrogels was monitored for 18 h in simulated gastrointestinal conditions. Dry hydrogels were weighted and placed in 20 mL simulated gastric fluid (SGF, *p*H 1.2) at 37 °C for 2 h, in a thermostated shaking bath with a rotational speed of 75 rpm. At specific time intervals the samples were removed from the solution and weighed again. After 2h the samples were transferred in 20 ml simulated intestinal fluid (SIF, *p*H 7.4) at 37 °C for 16 h. The extent of swelling degree was monitored by recording the weight of the hydrogels at specific intervals. The swelling degree was calculated using equation (1).

$$(W_t - W_0)/W_0 \cdot 100 \quad (1)$$

where W_t is the weight of swollen gels at time t and W_0 is the initial weight of samples. The swelling experiments were conducted in triplicate to minimize error and are reported as a mean value.

SEM analysis

A scanning electron microscope (SEM Quanta Inspect F) was employed to study the morphology of final hybrid materials using a sample cut in liquid nitrogen and sputtered with a thin layer of gold.

In vitro drug release

The drug release profile was determined in an automated dissolution USP Apparatus 1 (708-DS Agilent) with an autocotrolled multi-chanel peristaltic pump (810 Agilent), an UV/Vis spectrophotometer (Cary 60) with 1 mm flow cell and UV-Dissolution software. The hydrogels were immersed in 200 mL of dissolution medium at 37 °C. Rotational speed of 75 rpm was tested. The samples were maintained for 2 h in SGF followed by an immersion of 16 h in SIF. At specific time intervals the amount of released ASA was determined with a known concentration of the standard solutions at 277 nm in SGF and 267 nm in SIF. The ASA release mechanism from PVA-HNT films was determined by fitting the drug release profiles in different kinetic models: Zero order, First order, Higuchi, Korsmeyer-Pepas, Hixson-Crowell, Weibull. The best fitted model was determined by the regression coefficient (R^2)

Cell culture studies

Cell studies were conducted using fibroblast cell lines L929. The cells were maintained in the cell culture medium (DMEM) supplemented with 10% FBS, 100 μg penicillin, 100 u/mL streptomycin and 1 mM L-glutamine. Cells were incubated at 37°C in a 5% CO_2 incubator at an absolute relative humidity. After reaching 80-85 % confluence the cells were trypsinized and used for the assays.

Cell Viability Assay

The in vitro cytotoxicity of PVA, PVA-HNT 1%, PVA-HNT 5%, PVA-HNT 10% was evaluated by two different tests: indirect and direct contact. Prior to cell culture assays all samples were sterilized by soaking in 70% alcohol solution and shaking for 5 min, washed 3 times with 200 μL PBS and washed again with serum free medium 3 times at 30 min time interval to reach equilibrium. The indirect assay was realized as follows. The samples were short spin centrifuged in order to remove the PBS and then a 1:20 weight ratio of medium was added on the sample. The sample were incubated for 24 h under steering at 37°C. The 100 μL eluted medium was transferred over cells that were already seeded for 4h to attach in monolayer on a 96-well plate surface at a density of $8x10^4$ cell/mL. The control used for the indirect tests was complete medium and triton X100 solution with a final concentration of 0.02%. Serial binary solutions were used. For the direct test the samples were transferred over cells that were already seeded for 4h to attach in monolayer on a 96-well plate surface at a density of $8x10^4$ cell/ml and incubated for 24 h in normal conditions. As positive control TCP was used in similar conditions.

The metabolic activity of cell culture was quantified using 3-(4,5-dimethylthiazol-2-yl)-2,5-diphenyltetrazolium bromide (MTT) assay. Then the cells were treated with 10 μL/well MTT solution of 5mg/ml concentration and incubated again for 3 h in normal conditions. The culture medium was removed and 100 μL /well of DMSO were added to dissolve the formed formazan crystals. After the plate was shaken for 5 min, the optical density (O.D.) was read on a multiwell microplate reader (Tecan Nanaoquant infinite M200 PRO) at 570 nm wavelength.

Results and discussions

FTIR Analysis

The spectra of pure PVA, HNT and the three hybrid materials are shown in Fig. 1. Pure PVA exhibits typical bands of vinyl polymers. The bands from 2800-3000 cm^{-1} correspond to stretching vibrations of CH and CH_2 groups, while the bands attributed to CH and CH_2 deformation vibrations appear in 1300-1500 cm^{-1} range. Also, very broad hydroxyl bands appear at 3000-3600 cm^{-1} and accompanying C-O stretching from 1000-1260 cm^{-1}. The FTIR spectrum of the HNT exhibits two Al_2OH stretching bands at 3691 and 3616 cm^{-1} attributed to the OH bending that makes the connection between two Al atoms, a band at 1637 cm^{-1} assigned to the stretching vibration of OH groups from adsorbed and coordinated water, two bands at 1089 and 1029 cm^{-1} which correspond to Si-O-Si stretching vibration and a single Al_2OH bending band at 910 cm^{-1}. For the hybrid materials it can be observed a

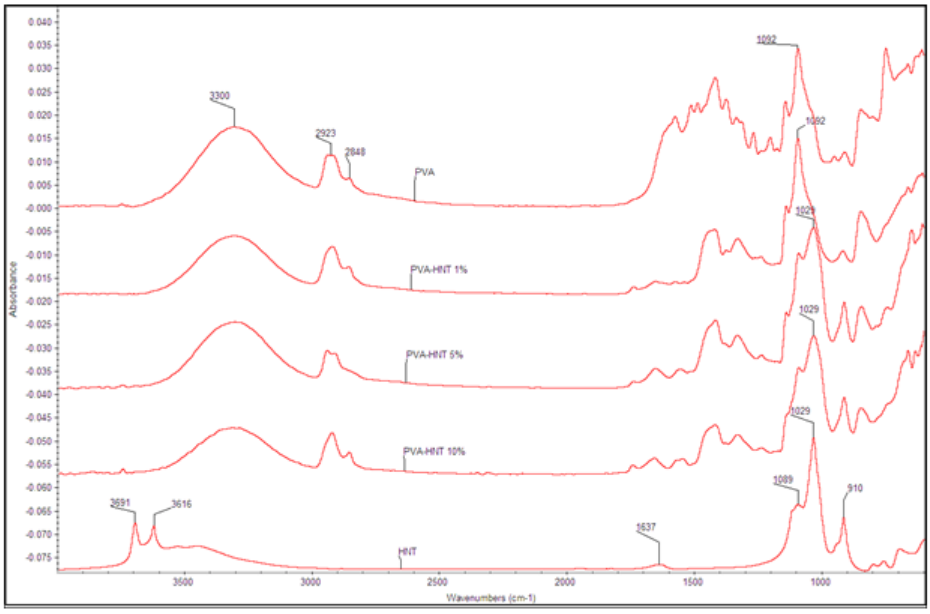

Fig. 1. FTIR spectra for PVA, HNT and PVA-HNT hysrogels

decrease of the intensity peak at 1092 cm^{-1}, assigned to C-O from PVA and an increase of the peak at 1029 cm^{-1} assigned to Si-O-Si from HNT as the HNT amount increases. This means that the addition of clay restrict the PVA chains mobility.

XRD Analysis

Figure 2 shows XRD spectra of pure PVA and hydrogels with different amounts of HNT. The pristine PVA exhibits a broad peak at 19.6°, a typical peak assigned to the semicrystalline structure of the polymer [38]. In the XRD spectrum of HNT, the peak from $2\theta=12°$ is characteristic to d_{001} crystallographic plane. For the composite with low amount of HNT (1 wt. %) the spectrum exhibits only the peak from PVA which means that the filler is homogenous dispersed within the polymer matrix. In the case of hybrid materials with 5 and 10 % HNT the peak from $2\theta=12°$ starts to appear and becomes more intense with the increase of HNT amount. This behaviour may be attributed to some agglomeration of HNT within the polymer matrix [39].

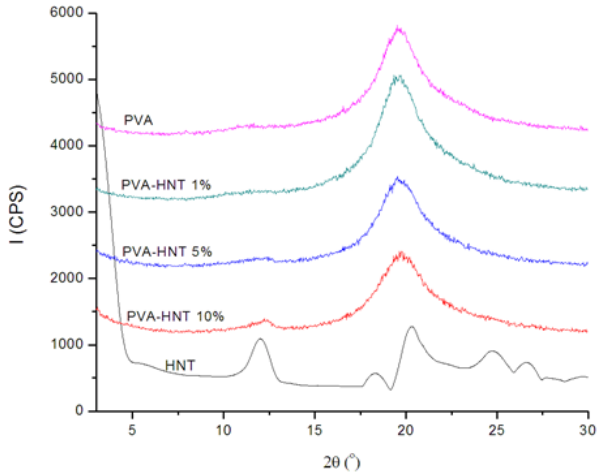

Fig. 2. XRD spectra for PVA, HNT and PVA-HNT hydrogels

Swelling Analysis

The swelling properties of hydrogels depend on the aluminosilicate content and the *p*H of the environment. It can be observed that in SGF the PVA-HNT hydrogels swell faster than the neat PVA hydrogel and also PVA-HNT 1% exhibit a higher swelling degree compared with PVA-HNT hydrogels with 5 and 10 wt. % HNT. This is due to the fact that the amount of negative charges in the hybrid material increases and the interaction between the water molecules and ionic group of the PVA is enhanced. By increasing the HNT content (5 wt.%, 10 wt.%) a denser cross-linking network is formed and the water adsorption capacity is limited [40].

After 24 h, the swelling degree of PVA –HNT 10% is lower than that of PVA hydrogel because PVA is not a pH sensitive polymer and so the water molecule diffuse through the polymer matrix while PVA-HNT 10 wt. % hydrogel contains a higher number of negative charges which lead to electrostatic repulsion between the hydrogel and SIF [41].

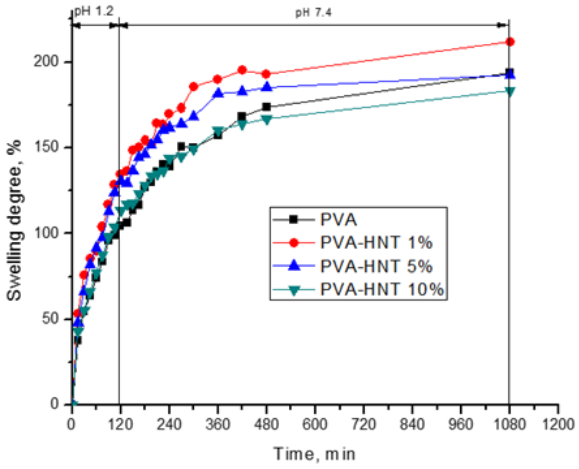

Fig.. 3. Effect of clay content on hydrogels swelling degree

SEM Analysis

The morphology of pristine PVA and PVA-clay hydrogels was characterized by SEM. From figure 4A it can be observed that the fractured surface of PVA hydrogel presents a wrinkled structure with fine parallel oriented wrinkles. In the case of the hydrogel with 1 wt. % HNT, the cross section (fig. 4B) becomes rough, due to the fact that the aluminosilicate is coated with polymer. Also the formation of large number of small cavities was observed. This explains the high swelling degree of PVA-HNT 1 wt. % hydrogel, more water molecules being absorbed within this cavities. For PVA-HNT 5% (fig. 4C) the morphology of the material is similar with the one of neat PVA hydrogel, wrinkled surface with few small agglomerations of the filler in some parts of the hydrogel being observed. Mostly, this material is characterized by a homogeneous dispersion

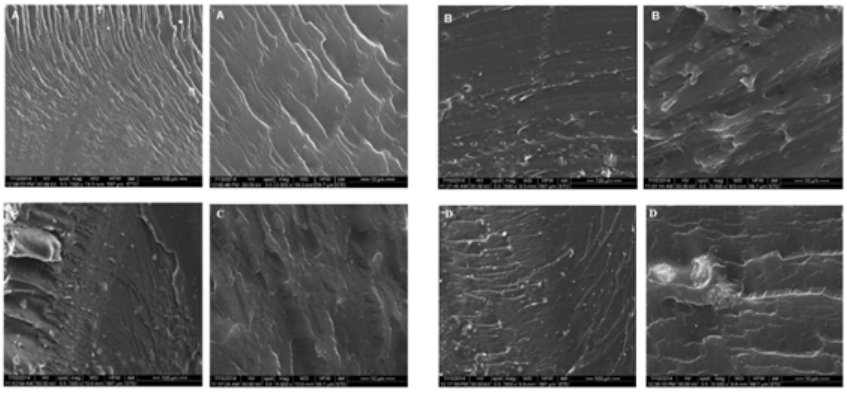

Fig.. 4. SEM images of: A) PVA; B)PVA-HNT 1%; C) PVA-HNT 5%; D) PVA-HNT 10% at different magnifications

of the aluminosilicate but it is not coated by the polymer. Only a few cavities can be observed and these explain the higher swelling degree rate compared with PVA hydrogel. Due to the similar morphology between the two materials after 24 h they reach the same swelling degree. PVA-HNT hydrogel with 10 wt.% HNT shows a similar morphology with PVA hydrogel, fine parallel wrinkles. Incorporation of 10 wt. % HNT within the polymer matrix leads to larger cluster formation, but there are also some areas where the aluminosilicate is homogenously dispersed.

In vitro drug release

In vitro release profiles of ASA from various hybrid materials in simulated gastrointestinal tract conditions are shown in figure 5. It can be observed that for hybrids based on HNT 1 wt.% and 5 wt.% the release rate is higher but for HNT 10 wt.% the lowest release rate in the first two hours (in SGF) was obtained. The same tendency was maintained in the first 4 h of releasing in SIF. After that the release rate of PVA-ASA is drastically reduced. All hybrid materials reached 100 % released drug in about 8-9 h while PVA-ASA released all the drug in 11 h. In the case of these hydrogels a high influence on drug release profile is the amount of negative charges presented on HNT surface.

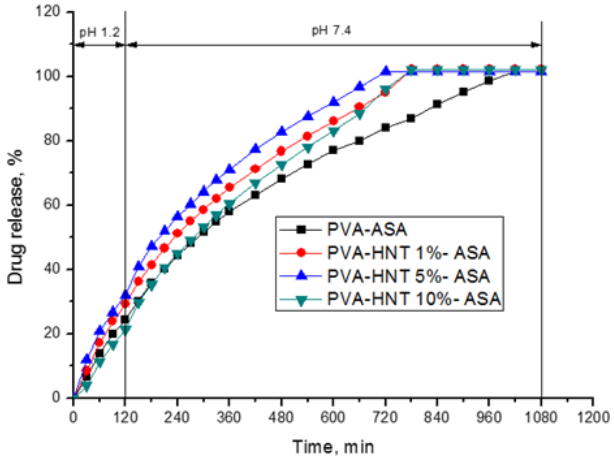

Fig.. 5. Release profile of ASA from different PVA-HNT hydrogels in simulated gastrointestinal conditions

The lower release rate for ASA from PVA-HNT 10% can be explained by cluster formation, confirmed by SEM analysis and by the formation of a denser crosslinking network, the drug being entrapped within it. These results suggest that these hybrid materials are suitable for oral administration.

In order to determine the release mechanism of ASA from PVA-HNT films in simulated intestinal fluids different mathematical models were considered being described by the following equations:

Zero order model: $Q_t = Q_0 + k_0 t$ (2)

First order model: $\log C = \log C_0 - {kt}/{2.303}$ (3)

Higuchi model: $Q = k_H \sqrt{t}$ (4)

Hixson-Crowell model: $\sqrt[3]{W_o} - \sqrt[3]{W_t} = k_{HC} t$ (5)

Korsmeyer-Pepas model: ${M_t}/{M_\infty} = k_{KP} t^n$ (6)

Weibull model: $\log[-\ln(1-m)] = b\log(t - T_t) - \log a$ (7)

where Q_t is the amount of drug dissolved in time t, Q_0 is the initial amount of drug in the solution, k_0 is the zero order release constant, C_0 is the initial concentration of drug, k is the first order rate constant, k_H is the Higuchi dissolution constant, W_0 is the initial amount of drug in the pharmaceutical dosage form, W_t is the remaining amount of drug in the pharmaceutical dosage form at time t, k_{HC} is a constant incorporating the surface volume relation, M_t/M_∞ is a fraction of drug released at time t, k_{KP} is the release rate constant and n is the release exponent, m is the accumulated fraction of the drug in dissolution medium at time t, a is the time scale of the process, Tt is the lag period before the onset of dissolution or release process, b if the shape parameter which characterizes the curves [42-44], the results being shown in table 1. Based on the data obtained for the release exponent from the linearization of the release profiles it can be confirm that ASA is released from the PVA films through a complex mechanism consisting of drug diffusion and polymer erosion. The release of ASA from PVA-HNT 1% and neat PVA films obeys the first order model (regression coefficient $R^2 > 0.99$). The release of ASA from the PVA-HNT 5% and PVA-HNT 10% films fits the zero order model (regression coefficient $R^2 > 0.99$) meaning that the drug release is not dependent of time. The release mechanism of ASA from the hydrogel films was determined with the Korsmeyer-Pepas model where the regression coefficient R^2 is higher than 0.98 in all case of the samples. Depending on the value of the n exponent, the release mechanism can be defined. If $n < 0.45$ the drug is released by the Fickian diffusion model. If $0.45 < n < 0.89$ the drug release follows an anomalous diffusion model that implies a combine diffusion and erosion mechanism. If $n = 0.89$ it appears the polymer relaxation and the drug follows the case II transport and if $n > 0.89$ the super case II transport takes place [45].

In table 1 there are also summarized the values of the release rate constant, k, the release exponent, n, and the regression coefficient, R^2 for Korsmeyer-Pepas model. The values of the release exponent indicate that the release of ASA from PVA-HNT 0%, PVA-HNT 1% and PVA-HNT 5% takes place by an anomalous diffusion, while from PVA-HNT 10% the release follows a super case II transport which implies the polymer relaxation and the swelling effect in simulated body fluids. The value of the kinetic constant, k_{HC}, obtained from Korsmeyer-Pepas model gives

		PVA-HNT 0%	PVA-HNT 1%	PVA-HNT 5%	PVA-HNT 10%
Zero order	Q_0	1.9584	3.4078	5.7184	12.424
	k_0	11.368	12.962	13.837	-1.961
	R^2	0.9947	0.9939	0.994	0.9945
First order	C_0	4.6064	4.6	4.5864	4.6501
	K	0.003396	0.076552	0.087234	0.068042
	R^2	0.9973	0.9981	0.9884	0.9897
Higuchi	k_H	16.756	20.145	22.904	14.945
	R^2	0.9214	0.9319	0.9567	0.8419
Hixson-Crowell	k_{HC}	0.2124	0.2575	0.2984	0.1988
	R^2	0.9966	0.995	0.9819	0.9763
Korsmeyer-Pepas	n	0.8349	0.7942	0.7947	1.0396
	k_{KP}	2.6449	2.8444	2.955	2.3961
	R^2	0.9973	0.9979	0.9906	0.9905
Weibull	a	-0.1738	-0.2164	-0.2613	-0.1443
	B	0.1998	0.2411	0.2704	0.211
	R^2	0.9364	0.9369	0.898	0.9002

Table 1
KINETICS OF ASA RELEASED FROM PVA-HNT FILMS

information regarding the release speed of drugs from the polymer matrix [46]. The results from table 1 indicate that the kinetic constant exhibits almost the same value for all hydrogels (k_{HC} varies between 2.39÷2.95) and therefore it may be concluded that the speed release of ASA from the hydrogels is not influenced by the presence of HNT within the polymer matrix.

Cell viability

In order to be used as drug delivery systems PVA-clay hydrogels need to exhibit no toxic effect. To determine pure PVA and PVA-HNT hydrogels cytotoxicity fibroblast cell lines L929 were used. In figure 6 the clay concentration influence on cell viability using MTT tests is shown. As can be observed from figure 6a the prim screening at indirect contact for 24 h of the hydrogels that contain different concentration of clays did not show major differences which may offer a conclusion about the cytotoxicity of the studied materials. Therefore the direct contact tests in the same conditions, with the same cell line type and the same cell concentration were done (fig. 6b). From figure 6b it may be noticed that the hydrogels which contain different amount of halloysite present a lower cell viability than the pristine PVA hydrogel and the TCP. By comparing PVA-HNT hydrogels, PVA-HNT 1% and PVA-HNT 5% show the highest cell viability probably because accordingly to SEM images HNT is finely dispersed within the polymer matrix. The lowest cell viability is observed on PVA-HNT 10% for which large clay clusters are formed and halloysite nanoparticle may diffuse in culture modifying the entire system and inducing a low toxicity. In good agreement with data reported by Zhou et.al. [47] PVA-HNT hydrogels are not cytotoxic suggesting that HNT exhibit good cyto-compatibility.

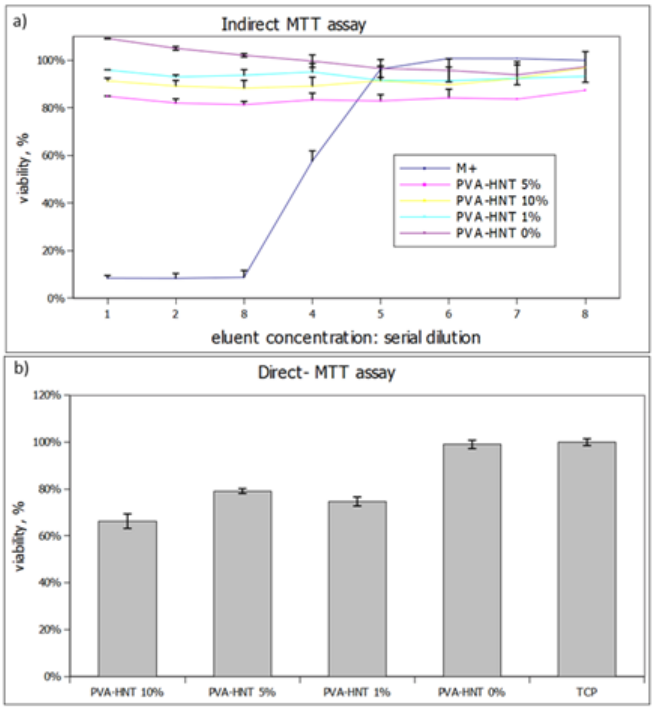

Fig. 6. MTT assays a) Indirect method and b) direct method

Conclusions

Various hydrogels based on PVA and different amount of HNT using a freeze-thawing method were synthesized. FTIR spectra show that adding of HNT within PVA matrix inhibits the chain mobility. A good dispersion of HNT added in low amounts was demonstrated by X ray diffraction. By increasing the HNT amount within the polymer matrix, some agglomerations of the aluminosilicate started to appear. This phenomenon has been observed also from SEM images. The concentration of HNT in PVA hydrogels exhibits a significant influence on swelling degree, a decrease of the swelling capacity of the hydrogels as the HNT concentration increases being observed. This is due to the hydrogen bonds formed between the OH groups from the PVA chains and the OH groups from HNT surface leading to a higher crosslinking degree. The in vitro release profile of ASA from the PVA-HNT hydrogels is also influenced by the HNT concentration. All drug delivery systems released 100 % of the drug. The faster release was gained for the hydrogels based on HNT, being due to the interactions between the negative charges from aluminosilicate surface and buffer solutions ions. The release of ASA from PVA-HNT hydrogels takes place by an anomalous or a super case II mechanism. The cytotoxicity tests indicate that if a high amount of clay is present in the hydrogels they become lightly toxic.

Acknowledgement: The work has been funded by the Sectoral Operational Programme Human Resources Development 2007-2013 of the Ministry of European Funds through the Financial Agreement POSDRU/159/1.5/S/132397.

References

1. BASU, S., DANDAPAT, M., GHOSH, D., MANDAL, D., Coloid. Surface A., 457, 2014, p. 196
2. KANGA, K.S., LEEB, S.I., HONG, J.M., LEE, J.W., CHOC, H.Y., SON, J.H., PAEK, S.H., CHO, D.W., J. Control. Release., 175, nr. 1, 2014, p. 10
3. NG, S.S., SU, K., LI, C., CHAN-PARK, M.B., WANG, D.A., CHAN, V., Acta Biomater., 8, nr. 1, 2012, p. 244
4. HUANG, C.J., DOSTALEK, J., KNOLL, W., Biosens. Bioelectron., 26, nr. 4, 2010, p. 1425-1431
5. OUN, R., PLUMB, J.A., WHEATE, N.J., J. Inorg. Biochem. 134, 2014, p. 100
6. LI, G., ZHANG, H., FORTIN, D., XIA, H., ZHAO, Y., Langmuir., 31, nr. 4, 2015, p. 11709
7. ASTON, R., WIMALARATNE, M., BROCK, A., LAWRIE, G., GRONDAHL, L., Biomacromolecules., 16, nr. 6, 2015, p. 1807
8.HILLBERG, A.L., OUDSHOORN, M., LAM, J.B.B. J.B.B., KATHIRGAMANATHAN, K., J. Biomed. Mater. Res., 103, nr. 3, 2016, p. 503
9. NOUAILHAS, H., EL GHZAOUI, A., LI, S., COUDANE, J., J. Appl. Polym. Sci., 122, nr. 3, 2011, p. 1599
10.BASRI, S.N., ZAINUDDIN, N., HASHIM, K., YUSOF, N.A., Carbohyd. Polym., 138, 2016, p. 34
11.DRAGAN, E.S., COCARTA, A.I., GIERSZEWSKA, M., Colloid. Surface. B., 139, 2016, p. 33
12.NGUYEN, N.T., LIU, J.H., Eur. Polym. J., 49, nr. 12, 2013, p. 4201
13. KENAWY, EL. R., KAMOUN, E.A., ELDIN, M.S.M., EL-MELIGY, M.A., Arabian J. Chem., 7, nr. 3, 2014, p. 372
14.MURAKAMI, T., SAKAI, N., YAMAGUCHI, T., YARIMITSU, S., NAKASHIMA, K., SAWAE, Y., SUZUKI, A., Tribol. Int., 89, 2015, p. 19
15.MEENAKSHI, AHUJA, M., Int. J. Biol. Macromol., 72, 2015, p. 931
16.YANG, L., MA, X., GUO, N., ZHANG, Y., Carbohydr. Polym., 105, 2014, p. 351
17. NAKAMURA, T., OGAWA, M., Appl. Clay Sci., 83-84, 2013, p. 469
18. PANIC, V.V., VELICKOVIC, S.J., Sep. Purif. Technol. 122, 2014, p. 384
19. ZANINI, V.P., LOPEZ DE MISHIMA, B., SOLÍS, V., Sens. Actuators. B., 155, no. 1, 2011, p. 75
20. POURJAVADI, A., AYYARI, M., AMINI-FAZL, M.S., Eur. Polym. J., 44, nr. 4, 2008, p. 1209
21. WANG, Q., ZHANG, J., WANG, A., J. Control. Release., 172, no. 1, 2013, p. e70
22. VIERA, K., JÁNOS, K., IVAN, K., JIRI, D., eXPRESS Polym. Lett., 7, no. 5, 2013, p. 471
23.LVOV, Y., AEROV, A., FAKHRULLIN, R., Adv. Colloid Iterface. Sci., 207, nr. 1, 2014, p. 189
24.ZHAO, Y., ABDULLAYEV, E., VASILIEV, A., LVOV, Y., J. Colloid Interface. Sci., 406, 2013, p. 121
25. GUO, B., ZOU, Q., LEI, Y., DU, M., LIU, M., JIA, D., Thermochim. Acta., 484, no. 1-2, 2009, p. 46
26. LECOUVET, B., GUTIERREZ, J.G., SCLAVONS, M.M., BAILLY, C., Polym. Degrad. Stab., 96,nr. 2, 2011, p. 226
27. MARNEY, D.C.O., RUSSELL, L.J., WU, D.Y., NGUYEN, T.V.X., CRAMM, D., RIGOPOULOS, N., WRIGHT, N.P., GREAVES, M.D., Polym. Degrad. Stab., 93,no. 10, 2008, p. 1971
28. ZHAI, R., ZHANG, B., WAN, Y., LI, C., WANG, J., LIU, J., Chem. Eng. J., 214, 2013, p. 304
29. BAI, H., ZHANG, H., HE, Y., LIU, J., ZHANG, B., WANG, J., J. Membr. Sci., 454, 2014, p. 220
30. XING, B., YIN, X.B., Biosens. Bioelectron., 24, nr. 9, 2009, p. 2939
31. LIU, M., ZHANG, Y., ZHOU, C., Appl. Clay Sci., 75-76, 2013, p. 52
32.RYBINSKY, P., JANOWSKA, G., Thermochim. Acta., 557, 2013, p. 24
33. DU, M., GUO, B., LEI, Y., LIU, M., JIA, D., Polymer., 49, no. 22, 2008, p. 4871
34. LEVIS, S.R., DEASY, P.B., Int. J. Pharma., 253, nr. 1-2, 2013, p. 145
35.VISERAS, M.T., AGUZZI, C., CEREZO, P., VISERAS, C., VALENZUELA, C., Micropor. Mesopor. Mater., 108, no. 1-3, 2008, 112-116.
36. WANG, Q., ZHANG, J., WANG, A., Appl. Surface Sci., 287, 2013, p. 54
37. TAN, D., YUAN, P., ANNABI-BERGAYA, F., LIU, D., WANG, L., LIU, H., HE, H., Appl. Clay Sci., 96, 2014, p. 50
38. PANDELE, A.M., IONITA, M., CRICA, L., DINESCU, S., COSTACHE, M., IOVU, H., Carbohydr. Polym., 102, 2014, p. 813
39. IP, K.H., STUART, B.H., THOMAS, P.S., RAY, A., Polym. Test., 30, nr. 7, 2011, p. 732
40. LI, P., KIM, N.H., SIDDARAMAIAH, LE, J.H., Compos. Part. B-Eng., 40, nr. 4, 2009, p. 275
41.BAO, Y., MA, J., SUN, Y., Carbohydr. Polym., 88, nr. 2, 2012, p. 589
42. MAITY, S., SA, B., AAPS Pharm. Sci. Tech., 2015, DOI: 10.1208/s12249-015-0359-0
43. FERREIRA, M., CHAVES, L., COSTA LIMA, S.A., REIS, S., Int. J. Pharm., 492, nr. 1-2, 2015, p. 65
44. JANGRA, S., GIROTRA, P., CHHOKAR, V., TOMER, V.K., SHARMA, A.K., DUHAN, S., J. Porous. Mat., 2016, p. 1
45. GHASEMNEJAD, M., AHMADI, E., MOHAMADNIA, Z., DOUSTGANI, A., HASHEMIKIA, S., Mat. Sci. and Eng. C., 56, 2015, p. 223
46. REHMAN, F., RAHIM, A., AIROLDI, C., VOLPE, P.L.O., Mat. Sci. and Eng. C., 59, 2016, p. 970
47. ZHOU, W.Y., GUO, B., LIU, M., LIAO, R., RABIE, A.B.M., JIA, D., J. Biomed. Mater. Res. A., 93A, nr. 4, 2010, p. 1574

Manuscript received: 23.03.2016